ARTICLE NO. 79-4113

Correlation Technique for Ambient Effects on Oxides of Nitrogen

R. M. Washam* and A. M. Mellor†
The Combustion Laboratory, Purdue University, West Lafayette, Ind.

Aircraft gas turbine engine testing requires large air flow rates and this is accomplished with ambient air. Daily changes in atmospheric air temperature, pressure, and humidity lead to variations in NO_xEI (g NO_x/kg fuel). A new scheme is proposed to correlate engine data and minimize this scatter due to changes in ambient conditions. The scheme is derivable from first principles; example calculations are shown for several Pratt and Whitney JT9D engines. The correlation technique is explained in detail, and the resulting scaling relation is discussed.

Nomenclature

A	= cross-sectional area
EI	= emissions index
k	= reaction rate coefficient
K	= equilibrium constant
l	= characteristic length
$\dot{m}$	= flow rate
M	= molecular weight of air
p	= pressure
R	= universal gas constant
t	= time
T	= temperature
V	= characteristic velocity
τ	= characteristic time
[ ]	= concentration

Superscripts

a	= order of pressure dependence

Subscripts

a	= air
apz	= primary zone air
$comb$	= combustor
f	= fuel
i	= inlet air
no	= nitric oxide
sl,no	= shear layer quenching for nitric oxide
$\phi = 1$	= stoichiometric

I. Introduction

EMISSIONS of oxides of nitrogen from conventional gas turbine engines are highly sensitive to the engine (and thus combustor) inlet air quality. Minor changes in water content, air temperature, and pressure create sizable variations in the peak combustion temperature, upon which NO_x has a high functional dependence. A review of selected ambient effect findings from the literature follows, along with a summary of a correlation technique capable of removing this dependence, with examples taken from JT9D engine certification tests.

Received Oct. 10, 1978; revision received March 23, 1979.

Index categories: Combustion and Combustor Designs; Environmental Effects.

*Graduate Instructor in Research, School of Mechanical Engineering; presently with Gas Turbine Division, General Electric Co., Schenectady, N.Y.

†Professor, School of Mechanical Engineering.

Lipfert[1] reduced scatter from several different engines significantly by decreasing NO_xEI 20% for each 0.01 (by weight) of water vapor in excess of 0.01 specific humidity. Carl,[2] in relating the fraction (NO_x at ambient humidity)/(NO_x level at a specific humidity of 0.005) vs percent specific humidity, obtained a straight line with a slope of -10.7%. In addition, it was suggested that ambient humidity has 60.7% the effect of water injection; thus, for a similar correlation in terms of water injection, a slope of -17.6% results. Also, Blazowski, Walsh, and Mach[3] provided a chart demonstrating the humidity effect on nitric oxides emission levels. A good summary of correlations is available from Rubins and Marchionna,[4] and Donovan and Cackette[5] have developed additional correlations.

In considering ambient temperature effects, Blazowski et al. developed a theoretical correction factor and expressed it in the form of a graph for pressure ratios of 10 to 25 and equivalence ratios of 0.6 to 0.9. Pressure variations generally are scaled with

$$NO_x \sim p^a \tag{1}$$

but a has been reported to vary from 0.13 to 1.5 by some workers,[4,6,7] while others recommend a constant value of 0.5.[8,9]

II. Background

A characteristic time correlation has evolved over the last several years which enables designers to estimate the effects of both combustor inlet conditions and combustor geometry on gaseous emissions. Originally qualitative,[10] this model has been applied successfully and quantified for laboratory burners,[11,12] automotive gas turbines,[11,13] helicopter combustors,[14] and the JT9D engine.[15] Although capable of correlating HC, CO, and NO_x emissions, it still has problems with the former two pollutants.[14,16] However, Hammond[16] has demonstrated the model's predictive ability for emissions of oxides of nitrogen. Here our attention will be limited to this pollutant.

The essence of the model is that NO forms only in the highest temperature regions of the combustor and that fuel nitrogen levels are very low.[14] We consider a near-stoichiometric eddy within the primary zone.[11,12] Zeldovich kinetics for thermal NO formation suggests that the rate of NO production in that eddy will be given by[17]

$$d[NO]/dt = 2k[O][N_2] \tag{2}$$

where the reaction in question is

$$O + N_2 \xrightleftharpoons{k} NO + N \tag{3}$$

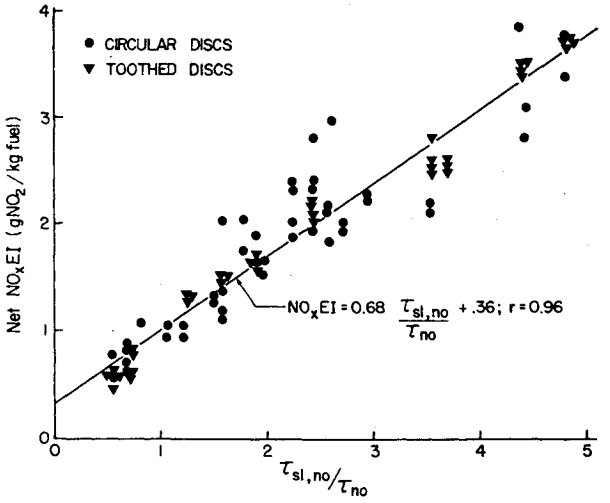

Fig. 1 NO_xEI correlation for C_3H_8 fuel for disk-in-duct burner.[11,12]

If it is assumed further that O/O_2 are in chemical equilibrium, then Eq. (2) becomes

$$d[NO]/dt = 2kK^{1/2}[O_2]^{1/2}[N_2] \tag{4}$$

Here K is the chemical equilibrium constant for the reaction

$$O_2 + M \overset{K}{\rightleftharpoons} 2O + M \tag{5}$$

The temperature dependence of Eq. (4) is Arrhenius and is given predominantly by $kK^{1/2}$:

$$kK^{1/2} \sim e^{-135{,}000\,\text{cal/mole}/RT_{\phi=1}} \tag{6}$$

Note that $T_{\phi=1}$ is a function of inlet air temperature and pressure, fuel type, and air humidity. Eq. (6) is specialized to $T_{\phi=1}$ since we argue that only near-stoichiometric eddies contribute substantially to NO formation.

The temperature dependence of Eq. (6) is correlated by a characteristic chemical time for NO formation, τ_{no}

$$\tau_{no} = 10^{-12} e^{135{,}000/RT_{\phi=1}} \text{ ms} \tag{7}$$

so that

$$d[NO]/dt \sim 1/\tau_{no} \tag{8}$$

Here the dependencies of the rate on oxygen and nitrogen concentration are neglected.

NO will form in the eddy of interest until secondary air is added and the reaction is quenched; this eddy lifetime is denoted $\tau_{sl,no}$ proportional to the ratio of a length scale (related to combustor geometry[13,14]) and the (fictitious) stoichiometric plug flow velocity through the combustor cross section:

$$\tau_{sl,no} = l_{no}/V_{\phi=1} \tag{9}$$

where

$$V_{\phi=1} = \dot{m}_{apz} RT_{\phi=1}/MpA_{comb} \tag{10}$$

By definition then, the total concentration of NO formed in the eddy is given by integration of Eq. (8) over the eddy lifetime

$$[NO]\,|_{\text{eddy}} \sim \int_0^{\tau_{sl,no}} dt/\tau_{no} \tag{11}$$

$$\sim \tau_{sl,no}/\tau_{no} \tag{12}$$

It is then assumed that the total number of NO-forming eddies is directly proportional to the total fuel flow rate:

$$[NO]\,|_{\text{total}} \sim \dot{m}_f \tau_{sl,no}/\tau_{no} \tag{13}$$

so that

$$NO_x\text{EI}\ (g\ NO_2/\text{kg fuel}) \sim \tau_{sl,no}/\tau_{no} \tag{14}$$

The proportionality constant in Eq. (12) is determined from experimental data, and the pre-exponential factor in Eq. (7)

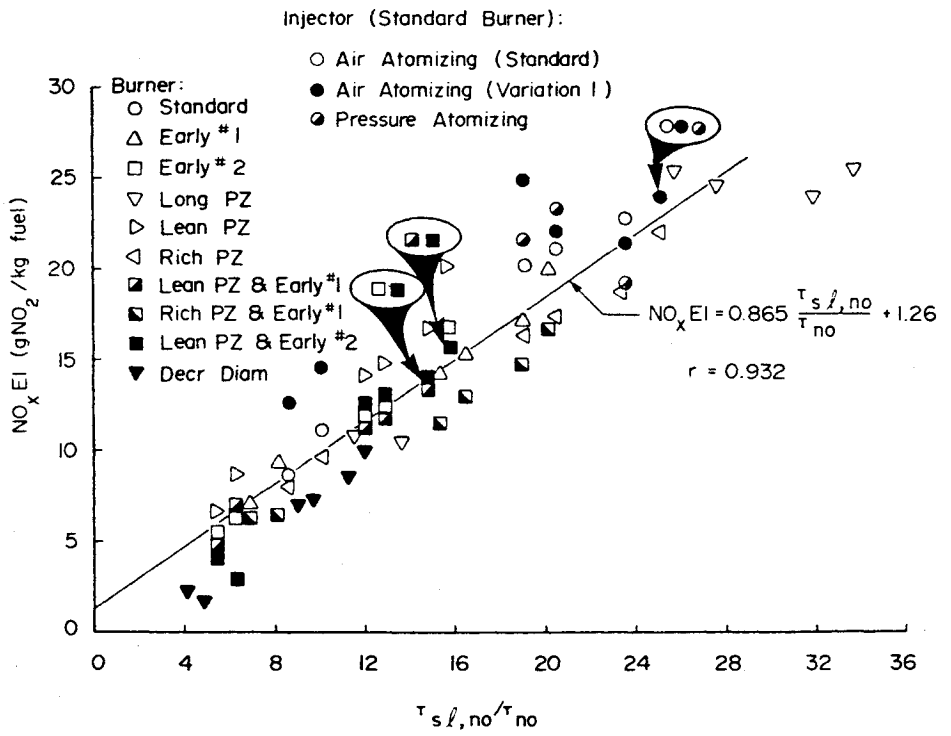

Fig. 2 NO_xEI goemetry and injector correlation for the automotive GT-309 burner.[13]

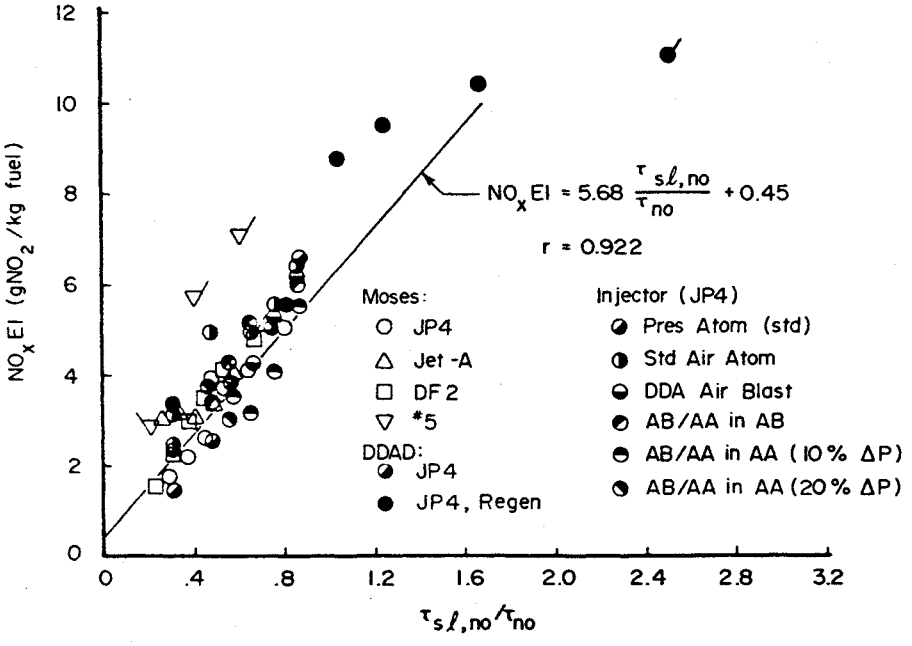

Fig. 3 $NO_x EI$ fuel and injector correlation for the helicopter T-63 burner.[14]

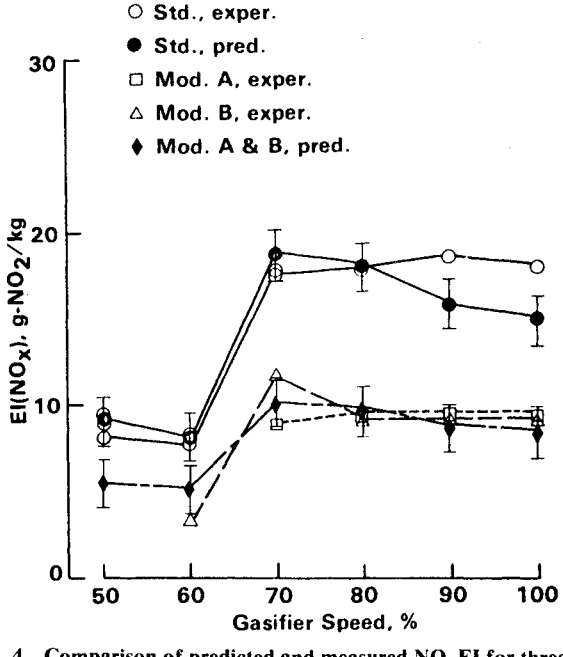

Fig. 4 Comparison of predicted and measured $NO_x EI$ for three GT-309 combustors.[16]

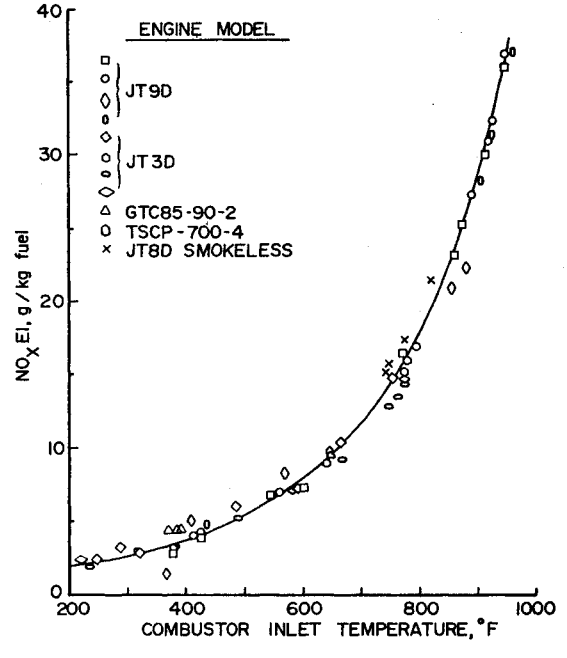

Fig. 5 Correlation of $NO_x EI$ with combustor inlet air temperature.[1]

has been selected to make the characteristic times of the same order. Examples of the correlation are given in Fig. 1 for a disk-in-duct laboratory combustor,[11,12] in Fig. 2 for the GT-309 automotive combustor,[11,13] and in Fig. 3 for the T-63 helicopter engine.[14] Note in this last figure that the model does not correlate the flagged triangles for a #5 oil containing fuel nitrogen. An example of the predictive capability is shown in Fig. 4 where the effect of geometry variations (modifications A and B) on NO_x is given to within one standard deviation.[16] The universality of the correlations is examined elsewhere.[15]

Equation (14) is useful in interpreting NO_x correlations available in the literature. Lipfert[1] found that a single curve fit a large number of engines when plotted against inlet air temperature (Fig. 5); Sawyer et al.[18] recast this as $ln(NO_x EI)$ vs $1/T_{\phi=1}$ and obtained an apparent activation energy of 136,000 cal/mole (the straight line in Fig. 6). From Eqs. (7) and (14)

$$\ell n(NO_x EI) \sim \ell n\tau_{sl,no} - \ell n\tau_{no} \tag{15}$$

$$\sim \ell n\tau_{sl,no} - \ell n 10^{-12} - 135{,}000/RT_{\phi=1} \tag{16}$$

which is a nearly identical result. Recall that $T_{\phi=1}$ is, as noted above, a function of inlet air temperature.

Equation (16) and Fig. 6 indicate that for engines correlated in Figs. 5 and 6, the $\tau_{sl,no}$'s must be nearly constant. This is roughly equivalent to stating that the ratio of combustor diameter to reference velocity is very similar for the engines in question, a reasonable result in view of accepted design practice for conventional burners.

Equation (14), shown consistent with literature correlations, will also allow inclusion of ambient effects: we consider each separately below.

The presence of water vapor will have its most significant effect upon the computed adiabatic stoichiometric flame temperature $T_{\phi=1}$ when this temperature (and thus $NO_x EI$)

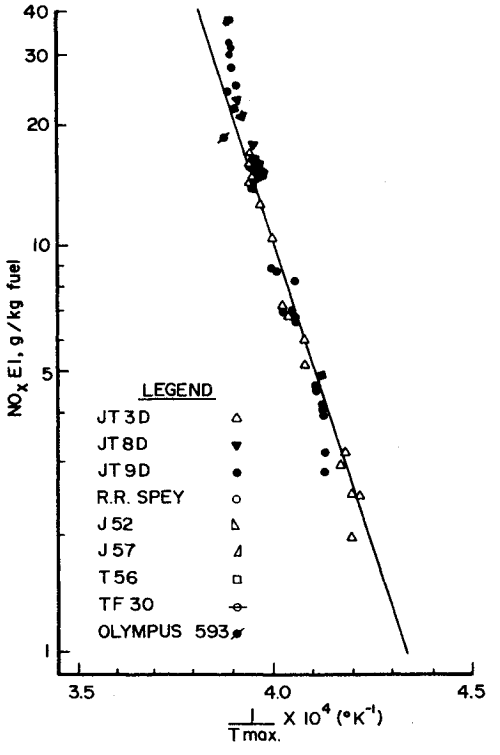

Fig. 6 Correlation of NO_xEI with stoichiometric adiabatic flame temperature, based on combustor inlet air temperature.[18]

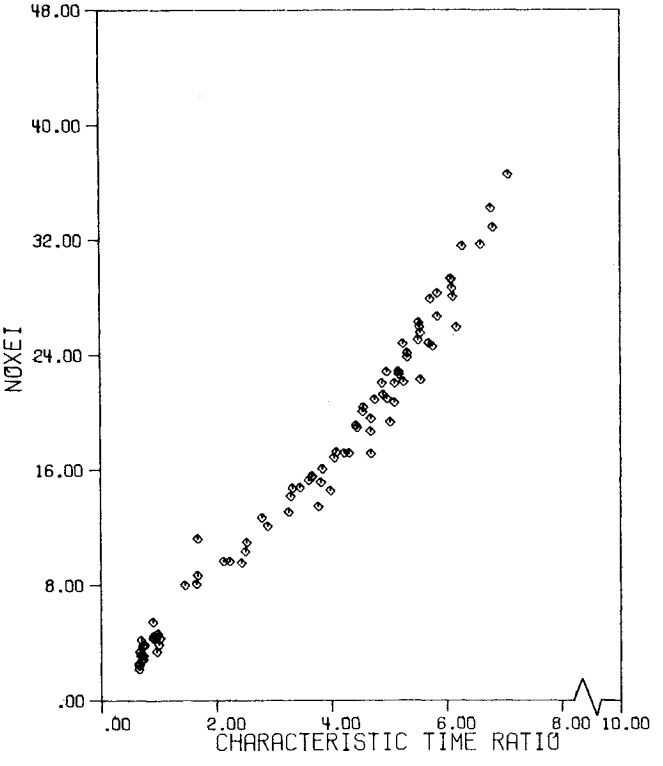

Fig. 7 Correlation of the JT9D NO_xEI data for one burner modification with one fuel.

Table 1 Temperatures calculated with measured inlet conditions[a]

Power[b]	$\dot{m}_a$, kg/s	p,atm	T_i, K	$T_{\phi=1}$, K
1	20.714	3.468	465.333	2368.000
2	21.988	3.687	470.889	2374.000
3	49.136	9.669	629.889	2471.000
4	58.412	11.909	669.000	2495.000
5	70.662	14.706	709.500	2520.000
6	78.957	16.838	736.722	2537.000
7	82.375	17.750	747.111	2544.000
8	85.703	18.653	756.000	2550.000
9	90.019	19.940	771.611	2559.000

[a] 0.0073 g H_2O/g. [b] Lowest fuel flow rate is arbitrarily labeled power 1.

Table 2 Temperatures calculated assuming zero humidity

Power	$\dot{m}_a$, kg/s	p,atm	T_i, K	$T_{\phi=1}$, K
1	20.714	3.468	465.333	2382.000
2	21.988	3.687	470.889	2386.000
3	49.136	9.669	629.889	2485.000
4	58.412	11.909	669.000	2509.000
5	70.662	14.706	709.500	2534.000
6	78.957	16.838	736.722	2550.000
7	82.375	17.750	747.111	2557.000
8	85.703	18.653	756.000	2562.000
9	90.019	19.940	771.611	2572.000

decreases as ambient humidity increases, since the inverse linear dependence (in $V_{\phi=1}$) in $\tau_{sl,no}$ will be overpowered by the exponential dependence in τ_{no}.

Ambient air temperature has a similar effect upon combustor inlet temperature and thus $T_{\phi=1}$. Increases in ambient temperature increase $T_{\phi=1}$ and NO_xEI through the exponential dependence in the kinetic time.

Any change in ambient pressure is reflected in the value of combustor inlet pressure appearing in Eq. (10) for $V_{\phi=1}$. NO_xEI is a direct function of p. A second order effect is that increases in p also increase $T_{\phi=1}$ through the suppression of equilibrium dissociation; as noted previously, this also leads to higher NO_xEI. In the next section, engine data used to test the correlation technique are discussed.

III. JT9D Engine Test Data

For the analysis to follow, the data were obtained by Pratt and Whitney Aircraft[19] during certification tests of eleven JT9D engines with Mod II burners operating on JP-4 fuel, over a period from September of 1973 to March of 1974. Engine inlet temperature and pressure, specific humidity, burner inlet temperature, pressure, fuel/air ratio and fuel flow rate, and NO_xEI were made available. (Other information that was provided is not relevant to the present study.) Including all day-to-day variations and correlating these data with Eq. (14) yields the fit shown in Fig. 7 and the least squares equation

$$NO_x EI = 4.554\tau_{sl,no}/\tau_{no} - 0.409 \qquad (17)$$

with a standard deviation in slope of 0.080 and a correlation coefficient $r = 0.987$.

IV. Ambient Effects

A sample calculation of the effect of humidity is shown in Tables 1 and 2 for one engine. The data in the former table are shown in Fig. 7 with the other engine data and were computed with the actual specific humidity (approximately 0.0073gH_2O/g air) measured by Pratt and Whitney. In Table 2 the flame temperatures, assuming no water vapor present in the inlet air, are presented. The effect of the triatomic H_2O replacing the diatomic N_2 in the air is the lower $T_{\phi=1}$ in Table 1, about a 13 K decrease. Similar calculations have been performed for all engines in Fig. 7 with the result shown in Fig. 8. As can be seen, the scatter is increased (standard deviation in slope to 0.082), and the correlation coefficient r has decreased to 0.983. The least squares fit equation for Fig. 8 is

$$NO_x EI = 4.133\tau_{sl,no}/\tau_{no} - 0.272 \qquad (18)$$

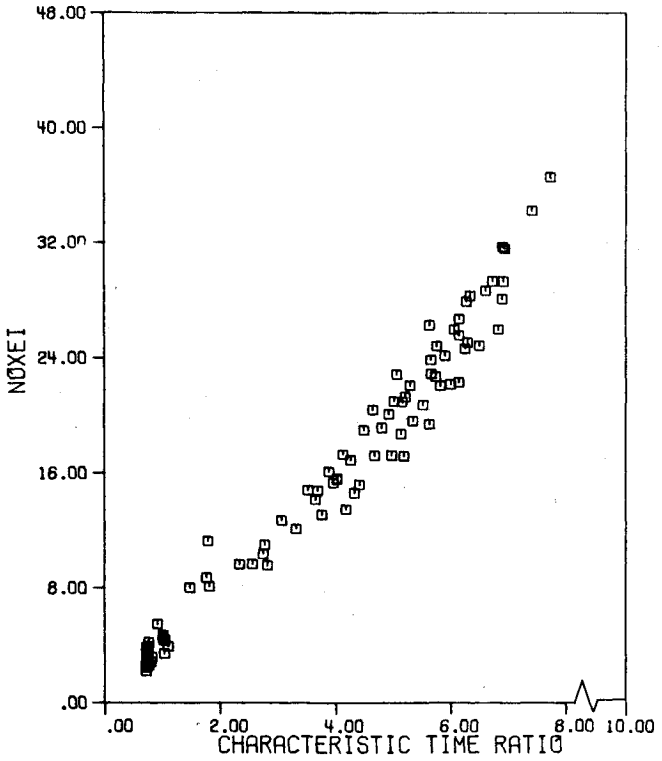

Fig. 8 Correlation of the JT9D NO_xEI data for one burner modification with one fuel and neglecting ambient humidity.

where the slope change from Eq. (17) reflects correlation of the same data with lower values of τ_{no}.

For ascertaining ambient temperature and pressure effects, a different approach was used. One engine, actually tested at 294 K and 0.99 atm, was selected. For the same pressure, engine inlet temperatures of 244 and 322 K were taken. (Combustor inlet tempertures were computed assuming a polytropic compression.) For each of these new burner inlet air tempertures and new adiabatic stoichiometric flame temperatures, Eq. (17) was used to compute the resulting NO_xEI. Figure 9 shows the significant changes which result from variations in ambient air temperature, compared with the baseline data obtained on a nearly standard day.

A similar method was utilized for ambient pressure. For the same engine, air temperature was held constant at 294 K, but inlet pressure was taken as 0.95 and 1.05 atm (baseline was 0.99 atm). The primary effect here is on p rather than TSTO, as noted previously. Figure 10 shows the computed changes in NO_xEI. Note that the model predicts a complicated pressure scaling parameter:

$$NO_x EI \sim p/T_{\phi=1}\tau_{no} \tag{19}$$

Again, the exponential dependence of τ_{no} will overcome the linear $T_{\phi=1}$ term. As pressure and $T_{\phi=1}$ increase, τ_{no} decreases, which suggests a greater than unity exponent (when including the variation in reference velocity with pressure).

As an additional note, humidity effects were analyzed and a semiempirical correction factor developed for the specific case of the JT9D combustor. NO_xEI was found to decrease by approximately 20% for each 1% increase in specific humidity; this represents a value of -20% for the correction factor.

This JT9D humidity correction factor of -20% agrees quite well with the literature. The magnitude of the factor is the same for water injection. In addition, for the appropriate operating pressure ratios, the correction factor is compatible with the predictions of Blazowski et al. However, the factor was developed for the JT9D and does not necessarily apply for other engines.

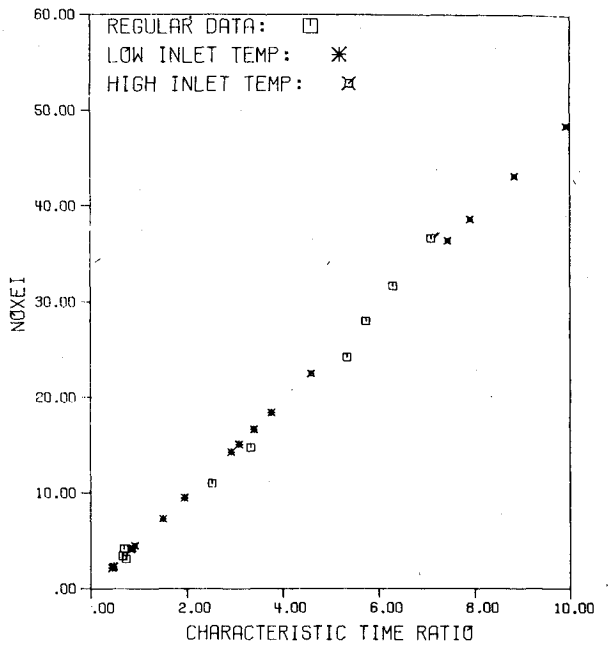

Fig. 9 Ambient temperature effect on NO_xEI.

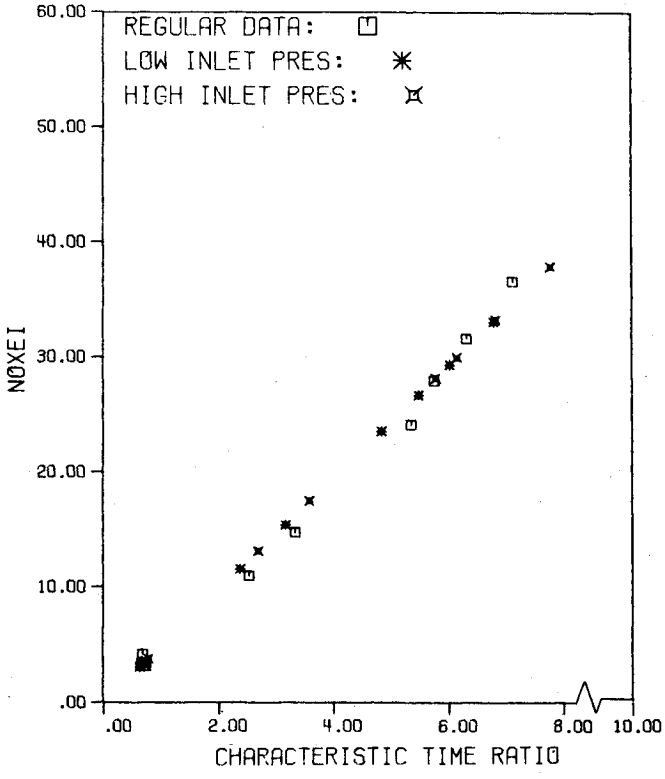

Fig. 10 Ambient pressure effect on NO_xEI.

In comparing the ambient pressure scaling results predicted by the model with the findings in the literature, there is an apparent discrepancy (see also Ref. 4). The model suggests that the exponential dependency of NO_xEI on pressure is of the first order, while the literature suggests that the exponent's value is around one-half. However, the exponent of one-half is a result of kinetic considerations only, whereas the model predicts pressure effects on reference velocity and the related variance of NO_xEI. Note also that, for constant reference velocity, the pressure dependence of $T_{\phi=1}$ and τ_{no} may explain the differing orders of pressure dependence reported by others.[4]

V. Summary

Equation (18) is the recommended scaling parameter for ambient temperature, humidity, and pressure variations. Substituting for τ_{no}

$$NO_x EI \sim (pe^{-67{,}976/T_{\phi=1}})/T_{\phi=1} \quad (20)$$

Here p is combustor inlet pressure and $T_{\phi=1}(K)$ is the adiabatic stoiciometric flame temperature (a function of ambient air properties and fuel heating value), computed assuming chemical equilbrium and utilizing actual ambient conditions to evaluate engine inlet conditions. Such calculations are time consuming, but since Eq. (19) is derivable from first principles, it may yield better correlations than purely empirical relations and should apply to any engine of any pressure ratio.

Acknowledgments

Financial support for this research was provided by the Environmental Protection Agency. The contents do not necessarily reflect the views and policies of the Environmental Protection Agency, nor does mention of trade names or commercial products constitute endorsement or recommendation. We appreciate R. Munt's support as grant monitor.

References

[1] Lipfert, F.W., "Correlation of Gas Turbine Emissions Data," ASME Paper 72-GT-60, March, 1972.

[2] Carl, D.E., "Influence of Ambient Humidity on Nitric Oxide Generation," *Gas Turbine International,* Vol. 15, May-June, 1974, pp. 28-32.

[3] Blazowski, W.S., Walsh, D.E., and Mach, K.D., "Operating and Ambient Condition Influences on Aircraft Gas Turbine NO_x Emissions," *Journal of Aircraft,* Vol. 12, 1975, pp. 110-115.

[4] Rubins, P.M. and Marchionna, N.R., "Evaluation of NO_x Prediction-Correlation Equations for Small Gas Turbines," AIAA Paper 76-612, 1976.

[5] Donovan, P. and Cackette, T., "The Effects of Ambient Conditions on Gas Turbine Emissions—Generalized Correction Factors," ASME Paper 78-GT-87, 1978.

[6] Mularz, E.J., Wear, J.D., and Verbulecz, P.W., "Pollution Emissions from Single Swirl-Can Combustor Modules at Parametric Test Conditions," NASA TM X-3167, Jan. 1975.

[7] Mularz, E.J., Wear, J.D., and Verbulecz, P.W., "Pollution Emissions from Single Swirl-Can Module Arrays at Parametric Test Conditions," NASA TM X-3237, June 1975.

[8] Fenimore, C.P., Formation of Nitric Oxide in Premixed Hydrocarbon Flames," Thirteenth Symposium (International) on Combustion, The Combustion Institute, Pittsburgh, Pa., 1970, pp. 373-380.

[9] Vermes, G., "A NO_x Correlation Method for Gas Turbine Combustors Based on NO_x Formation Assumptions," ASME Paper 74-WA/GT-10, 1974.

[10] Mellor, A.M., "Gas Turbine Pollution," *Progress in Energy and Combustion Sciences,* Vol. 1, 1976, pp. 111-133.

[11] Tuttle, J.H., Colket, M.B., and Mellor, A.M., "Characteristic Time Correlation of Emissions from Conventional Aircraft Type Flames," School of Mechanical Engineering, Purdue University, Rept. PURDU-CL-76-05, 1976.

[12] Tuttle, J.H., Colket, M.B., Bilger, R.W., and Mellor, A.M., "Characteristic Times for Combustion and Pollutant Formation in Spray Combustion," Sixteenth Symposium (International) on Combustion, The Combustion Institute, Pittsburgh, Pa., 1977, pp. 209-219.

[13] Mellor, A.M., "Characteristic Time Emissions Correlations and Sample Optimization: the GT-309 Gas Turbine Combustor," *Journal of Energy,* Vol. 1, July-Aug. 1977, pp. 244-249.

[14] Mellor, A.M., "Characteristic Time Emissions Correlations: the T-63 Helicopter Gas Turbine Engine," *Journal of Energy,* Vol. 1, July-Aug. 1977, pp. 257-262.

[15] Mellor, A.M. and Washam, R.M., "Characteristic Time Correlations of Pollutant Emissions from an Annular Gas Turbine Combustor," ASME Paper 79-GT-194, 1979.

[16] Hammond, D.C., "Evaluation of Characteristic Time Model Emissions Predictions for Three GT-309 Vehicular Gas Turbine Combustors," *Journal of Energy,* Vol. 1, July-Aug. 1977, pp. 250-256.

[17] Bowman, C.T., "Kinetics of Pollution Formation and Destruction in Combustion," *Progress in Energy and Combustion Science,* Vol. 1, 1976, pp. 33-45.

[18] Sawyer, R.F., Cernansky, N.P., and Oppenheim, A.K., "Factors Controlling Pollutant Emissions from Gas Turbine Engines," *Atmospheric Pollution by Aircraft Engines,* AGARD CP No. 125, 1973.

[19] Nelson, A.W., personal communication, Pratt and Whitney Aircraft, to R. Munt, Environmental Protection Agency, Oct. 1976.